Author Manuscript

Author Manuscript

Author Manuscript

Author Manuscript

HHS Public Access

Author manuscript

ACS Biomater Sci Eng. Author manuscript; available in PMC 2018 March 13.

Published in final edited form as:

ACS Biomater Sci Eng. 2017 March 13; 3(3): 409–419. doi:10.1021/acsbiomaterials.6b00663.

Prevention of Oxygen Inhibition of PolyHIPE Radical Polymerization using a Thiol-based Crosslinker

Michael E Whitely[1,+], **Jennifer L. Robinson**[1,+], **Melissa C. Stuebben**[1], **Hannah A. Pearce**[1], **Madison A.P. McEnery**[1], and **Elizabeth Cosgriff-Hernandez**[1,2,*]

[1]Department of Biomedical Engineering, Texas A&M University, College Station, Texas, 77843-3120, U.S.A.

[2]Center for Infectious and Inflammatory Diseases, Texas A&M Health Science Center, Houston, Texas, 77030, U.S.A

Abstract

Polymerized high internal phase emulsions (polyHIPEs) are highly porous constructs currently under investigation as tissue engineered scaffolds. We previously reported on the potential of redox-initiated polyHIPEs as injectable bone grafts that space fill irregular defects with improved integration and rapid cure. Upon subsequent investigation, the radical-initiated cure of these systems rendered them susceptible to oxygen inhibition with an associated increase in uncured macromer in the clinical setting. In the current study, polyHIPEs with increased resistance to oxygen inhibition were fabricated utilizing a tetrafunctional thiol, pentaerythritol tetrakis(3-mercaptoproprionate), and the biodegradable macromer, propylene fumarate dimethacrylate. Increased concentrations of the tetrathiol additive provided improved oxygen resistance as confirmed by polyHIPE gel fraction while retaining the requisite rapid cure rate, compressive properties, and pore architecture for use as an injectable bone graft. Additionally, thiol-methacrylate polyHIPEs exhibited increased degradation under accelerated conditions and supported critical markers of human mesenchymal stem cell activity. In summary, we have improved upon current methods of fabricating injectable polyHIPE grafts to meet translational design goals of improved polymerization kinetics under clinically relevant conditions without sacrificing key scaffold properties.

Graphical abstract

[*]Corresponding author: Dr. Elizabeth Cosgriff-Hernandez, Department of Biomedical Engineering, Texas A&M University, 5045 Emerging Technologies Building, 3120 TAMU, College Station, TX 77843-3120, Tel: (979) 845-1771, Fax: (979) 845-4450, cosgriff.hernandez@tamu.edu.

[+]5045 Emerging Technologies Building, 3120 TAMU, College Station, TX 77843-3120, Tel: (979) 845-9368, Fax: (979) 845-4450 Co-first authors

SUPPORTING INFORMATION

Quantification of polyHIPE pore size for PFDMA, PFDMA-5T, and PFDMA-10T.

NMR characterization of polyHIPE extracts for PFDMA and PFDMA-10T.

Author Manuscript
Author Manuscript
Author Manuscript
Author Manuscript

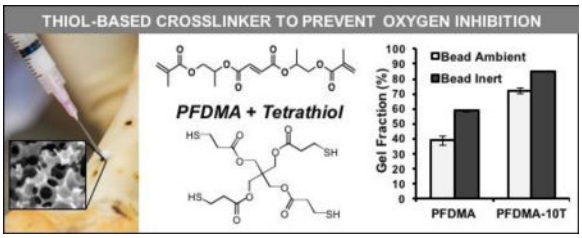

Keywords

THIOL-METHACRYLATE; POLYHIPES; SCAFFOLDS; MESENCHYMAL STEM CELLS

INTRODUCTION

Tissue engineers have demonstrated the importance of biomaterial scaffolds in guiding tissue regeneration.[1] Ideally, these scaffolds promote neotissue formation by providing a 3D substrate to guide cell growth, exhibiting requisite mechanical properties to restore function, and degrading at a rate that complements the rate of neotissue formation. A variety of fabrication strategies have been employed to achieve this diverse set of criterion with differing levels of success.[2–8] Emulsion templating is a unique fabrication technique that is currently being investigated for application in tissue engineering.[9–14] High internal phase emulsions (HIPEs) are characterized by an internal droplet phase volume fraction greater than 74%. Polymerization of the continuous phase secures the architecture defined by the emulsion geometry resulting in a high porosity foam (polyHIPE). Multiple compositional and processing variables have been investigated to determine the effect on emulsion stability and the corollary impact on the resulting pore architecture and mechanical properties. Through manipulation of these variables, a diverse set of scaffolds have been fabricated with a broad range of pore sizes, porosities, and mechanical properties that illustrate the utility of polyHIPEs for hard and soft tissue repair.[9–10, 12, 15–17]

Recently, our lab developed a polyHIPE scaffold for use as an injectable bone graft based on propylene fumarate dimethacrylate (PFDMA).[10] Unlike traditional poly(methyl methacrylate) bone cements, fumarate based polyHIPEs do not exhibit significant exotherms during polymerization and allow for hydrolytic degradation *in vivo*. Uniquely, these injectable grafts cure *in situ* to compressive properties approaching cancellous bone while also promoting osteogenic differentiation of human mesenchymal stem cells.[13] No previously investigated polyHIPE graft has displayed this combination of properties while retaining the requisite properties to permit deployment as a space-filler with *in situ* cure. Although initial *in vitro* testing of these scaffolds has proved promising, additional criteria need to be addressed to permit successful implementation in the clinic. A rapidly curing polyHIPE is desired to reduce surgical times, limit infection risk, and rapidly stabilize defects.[18] We recently reported a redox initiated polymerization route that improved upon previous methods of fabricating injectable polyHIPE grafts.[12] This system permitted fabrication of an off-the-shelf graft with long term storage and cure rates similar to commonly used bone cements (<15 minutes) without sacrificing porosity or compressive properties.

Author Manuscript Author Manuscript Author Manuscript Author Manuscript

The ability to achieve rapid cure with tunable polymerization profiles is a primary advantage of our polyHIPE system. However, an injectable polyHIPE for use as a bone graft must retain these characteristics when administered in the surgical suite, which includes exposure to an oxygen-rich environment. The utilization of radical mediated chain-growth polymerization of methacrylate-capped macromers in our scaffold design renders it susceptible to oxygen inhibition. Under oxygen-rich conditions, high levels of initiating and propagating radicals are scavenged and converted to peroxy radicals.[19–20] These peroxy radicals do not readily reinitiate polymerization of vinyl macromers, terminating further network formation. This often results in reduced cure rates, elevated levels of uncured macromer, and a reduction in mechanical properties.[21] Traditional industrial methods utilized to prevent oxygen inhibition (e.g. purging with inert gases) are not suitable to the proposed application as an injectable graft. Several researchers have reported reduced oxygen inhibition in thiol-ene and thiol-acrylate polymerizations. Thiol–acrylate and thiol-methacrylate polymerization may be initiated via hydrogen abstraction from a thiol functional group or radical addition to the acrylate/methacrylate functional group. Propagation then proceeds via thiol or methacrylic/acrylic radical addition to methacylate/acrylate functional groups.[22–25] Unlike vinyl systems where oxygen scavenges and effectively terminates radicals, the peroxy radicals generated in the presence of oxygen can abstract the thiol hydrogen to generate thiyl radicals that can continue to propagate through addition or chain transfer. Thus, the mixed mode initiation of the thiol-acrylate /methacrylate polymerizations renders them less susceptible to oxygen inhibition. It has been reported that increasing thiol monomer content in diacrylate systems resulted in reduced levels of oxygen inhibition.[25] Furthermore, higher thiol functionality provided a faster polymerization rate and increased viscosity, serving to further reduce diffusion of inhibitory oxygen. We hypothesized that the addition of a thiol-based crosslinker would confer resistance to oxygen inhibition under physiological environments to our injectable polyHIPE system. Although there are previous reports of thiol-methacrylate and thiol-ene polyHIPE systems, these were not injectable systems and did not characterize the effect of the thiol monomer on oxygen inhibition.[26–28]

In this study, we explore the use of a tetrafunctional thiol, pentaerythritol tetrakis(3-mercaptoproprionate (tetrathiol), to provide improved resistance to oxygen inhibition to injectable PFDMA polyHIPEs. Rheological properties were monitored to determine the effect of thiol on crosslinking kinetics by characterizing work and set times. To further probe this relationship, gel fraction was quantified to assess the impact of tetrathiol incorporation on network formation under ambient and inert conditions. To evaluate the potential of our system in orthopaedic applications, the effects of tetrathiol concentration on pore architecture, compressive modulus, and yield strength were assessed. Thiol based scaffolds have previously demonstrated improved degradation rates *in vivo* and could prove a potent method for tuning polyHIPE degradation. To this end, the effect of thiol incorporation on hydrolytic degradation rate was determined by measuring mass loss after accelerated hydrolytic testing. Finally, human mesenchymal stem cell (hMSC) activity and scaffold-induced osteogenic differentiation were investigated using established viability, proliferation, and alkaline phosphatase (ALP) assays. This work aims to highlight the strong

Author Manuscript Author Manuscript Author Manuscript Author Manuscript

potential of thiol-methacrylate polyHIPEs to serve as rapid-curing injectable bone grafts that retain desirable properties when applied under physiological conditions.

MATERIALS AND METHODS

Materials

Polyglycerol polyricinoleate (PGPR 4125) was donated by Palsgaard. Human mesenchymal stem cells were provided by the Texas A&M Health Science Center College of Medicine Institute for Regenerative Medicine at Scott & White. All other chemicals were purchased and used as received from Sigma–Aldrich, unless otherwise noted.

PFDMA Synthesis and Purification

Propylene fumarate dimethacrylate (PFDMA) was synthesized in a two-step process adapted from Timmer et al [29]. Briefly, propylene oxide was added dropwise to a solution of fumaric acid and pyridine in 2-butanone (2.3:1.0:0.033 mol) and refluxed at 75°C for 18 hours. Residual propylene oxide and 2-butanone were removed through a two-step distillation procedure. Residual acidic by-products and water were removed with washing, and the product was dried under vacuum (<0.2 millibar) at ambient temperature for 12 hours. The diester bis(1,2 hydroxypropyl) fumarate product was then end-capped with methacrylate groups using methacryloyl chloride in the presence of triethylamine. The molar ratios of the diester, methacryloyl chloride, and triethylamine were 1:2.1:2.1, respectively. Hydroquinone was added at a molar ratio of 0.008:1 to inhibit crosslinking during synthesis. The reaction was maintained below −10°C to reduce undesirable side reactions and stirred vigorously overnight under a nitrogen blanket. The macromer was neutralized overnight with 2 M potassium carbonate and residual base removed with an aluminum oxide column (7 Al_2O_3:1 TEA). The PFDMA product was then vacuum dried and the structure confirmed using ^{1}H NMR (300 MHz, $CdCl_3$), δ 1.33 (dd, 3H, CH3), 1.92 (s, 3H, CH3), 4.20 (m, 2H, -CH2-), 5.30 (m, 1H, -CH-), 5.58 (s, 1H, -C=CH2), 6.10 (s, 1H, -C=CH2), 6.84 (m, 2H, -CH=CH-). The integration ratio of methacrylate protons to fumarate protons in the ^{1}H NMR spectra was used to confirm > 90% functionalization prior to polyHIPE fabrication.

PolyHIPE Fabrication

HIPEs were prepared using a FlackTek Speedmixer DAC 150 FVZ-K following a method adapted from Moglia et al.[12] Briefly, PFDMA was mixed with a varied amount of pentaerythritol tetrakis(3-mercaptoproprionate) (0, 5, or 10 mol%) and 200 PPM hydroquinone as inhibitor, Figure 1. Two mixtures containing either 1 wt% benzoyl peroxide as initiator or 1 wt% trimethylaniline as reducing agent were combined with the organic phase and 10 wt% PGPR prior to emulsification. After homogenous mixing of the organic phase, an aqueous solution of calcium chloride (1 wt%) was added to the organic phase (75% v) in six additions and mixed at 500 rpm for 2.5 min. HIPEs were placed into a double barrel syringe and the two components mixed upon injection using a static mixing head into centrifuge tubes (5 mL syringe with 3 cm straight mixer, Sulzer Mixpac K-System). HIPEs were placed in a 37°C aluminum bead bath to facilitate crosslinking overnight.

Author Manuscript Author Manuscript Author Manuscript Author Manuscript

Rheological Analysis

Work and set times of the polyHIPEs were characterized using an Anton Paar MCR 301 rheometer following a procedure adapted from Foudazi et al.[30] Storage and loss moduli were measured every 15 seconds using a parallel-plate configuration with a 1 mm gap and 0.5% strain. Redox initiated HIPEs were injected through a mixing head onto the plate heated to 37°C. Work time was determined as the onset of storage modulus increases and set time determined as the tan δ minimum, which corresponds to the yielding of storage modulus. Values were reported as the average of three specimens from three different HIPEs for each composition (n = 9).

Gel Fraction and Sol Fraction Composition

Gel fraction was quantified to assess the impact of tetrathiol incorporation on network formation under ambient and inert conditions. Two distinct polyHIPE specimen morphologies were utilized to investigate the extent of oxygen inhibition during polymerization. To characterize network formation at the scaffold surface, polyHIPEs were cured into a bead morphology with a high surface-area-to-volume ratio under ambient conditions. Scaffolds were also cured in the same morphology under a nitrogen blanket to confirm inhibition by oxygen (Labconco Controlled Atmosphere Glovebox). To characterize network formation under bulk-cured conditions, polyHIPEs were cured into 15 mL centrifuge tubes and sectioned 1 mm thick from the polyHIPE bulk (Isomet® saw). All specimens were vacuum dried for 48 hours, weighed, and then extracted in dichloromethane (DCM) at a ratio of 1 mL DCM to 10 mg of specimen to facilitate dissolution of uncrosslinked macromer. After extraction on a shaker table for 48 hours, the DCM was decanted and the specimens vacuum dried for 48 hours at ambient temperature. The gel fraction was calculated as the final weight divided by original weight (n = 6). The fraction of mass loss attributed to surfactant was subtracted prior to gel fraction calculation. The extractables of high surface area bead constructs cured under ambient conditions were analyzed with ^{1}H NMR (300 MHz, $CdCl_3$) after vacuum removal of the DCM from the sol fraction. The integration ratio of the PFDMA methacrylate protons to tetramethylsilane protons in the ^{1}H NMR spectra was used to identify qualitative differences in residual monomer content present in 0 and 10 mol% thiol-methacrylate polyHIPEs.

Scaffold Architecture Characterization

Average polyHIPE pore size was determined using scanning electron microscopy (SEM, Phenom Pro, Nanoscience Instruments). Specimens from three separate polyHIPEs were vacuum dried for 24 hours to remove water, sectioned into disks, and fractured at the center to produce an unaltered surface for characterization. Each specimen was coated with gold and imaged in a raster pattern yielding five images. Pore size measurements were completed on the first ten pores that crossed the median of each 1000x magnification micrograph. Average pore sizes for each polyHIPE composition were reported (n = 150). A statistical correction was calculated to account for the random fracture plane through spherical voids and pores, $2/\sqrt{3}$.[31] Average diameter values were multiplied by this correction factor to yield a more accurate pore diameter description.

Author Manuscript Author Manuscript Author Manuscript Author Manuscript

Compressive Testing

The effect of thiol concentration on polyHIPE compressive modulus and yield strength was investigated following ASTM D1621-04a. PolyHIPEs were cured in 15 ml centrifuge tubes and sectioned into disks with a 3:1 diameter to height ratio (15 mm diameter, 5 mm thick) using an Isomet® saw. PolyHIPE specimens were compressed using an Instron 3300 at a strain rate of 50 mm/s. The compressive modulus was calculated from the slope of the linear region and the compressive strength was identified, after correcting for zero strain, as the stress at the yield point or 10% strain, whichever point occurred first. Reported compressive moduli and yield strength data were averages of nine specimens for each polyHIPE composition.

Accelerated Degradation In Vitro

Accelerated degradation testing was performed on polyHIPE specimens that were sectioned using an Isomet® saw into 1 mm thick sections. Specimens were vacuum dried for 48 hours and dry weights recorded prior to incubation in base solution (0.25 and 0.5M NaOH) at a ratio of 1 g specimen to 20 mL solution. Specimens were secured with Teflon weights in the solution and placed on a shaker table at 37°C. The solutions were changed every 2–3 days with time points every week for four weeks. At each time point, specimens were washed twice with RO water, incubated for 1 hour with 1 mL RO water to remove any salts and dried under vacuum for 48 hours before weighing (n = 3).

Culture of Human Mesenchymal Stem Cells

Bone marrow-derived hMSCs were obtained as passage 1 from the Center for the Preparation and Distribution of Adult Stem Cells at Texas A&M Health Science Center College of Medicine, Institute for Regenerative Medicine at Scott & White through NIH Grant # P40RR017447. Cells were cultured to 80% confluency on tissue-culture polystyrene flasks in standard growth media containing Minimum Essential Media α (MEM α, Life Technologies) supplemented with 16.5% fetal bovine serum (FBS, Atlanta Biologicals) and 1% L-glutamine (Life Technologies) prior to passaging. All experiments were performed with cells at passage 3.

Cytocompatibility of Leachable Components from PolyHIPEs

A viability study was performed to assess the cytocompatibility of the extractables from cross-linked polyHIPE networks immediately following scaffold injection and cure. PolyHIPEs containing 0 or 10 mol% tetrathiol were cured into a bead morphology with a high surface-area-to-volume ratio under ambient conditions and incubated in standard growth media at 37°C at a ratio of 0.13 mL HIPE to 1 mL media (surface area ~975 cm^2/mL). After 24 hours, the extraction media was collected and sterile filtered. To approximate the extractables from bulk-cured specimens that have roughly 50% of the sol fraction of the bead specimens, extracts were diluted to 0.5 vol% with media. hMSCs were seeded at a density of 40,000 cells/cm^2 in a 96-well plate and allowed to adhere for 24 hours prior to extract exposure. 100 μL of the extract solutions was added to hMSCs and the cells cultured for 24 hours. Viability was assessed utilizing the LIVE/DEAD assay kit (Molecular Probes) according to standard protocols. Briefly, cells were washed with PBS, stained with 2 μM

Author Manuscript Author Manuscript Author Manuscript Author Manuscript

calcein-AM (live) and 2 μM ethidium homodimer-1 (dead) for 30 minutes at 37°C, and washed with PBS for imaging. Imaging (3 images per specimen) was conducted on five specimens (n = 15) with a fluorescence microscope (Nikon Eclipse TE2000-S).

hMSC Viability on Thiol-Methacrylate PolyHIPEs

Investigation of hMSC viability and morphology on seeded constructs was performed to assess the effect of tetrathiol addition on cell behavior. PolyHIPEs were fabricated utilizing 0 or 10 mol% tetrathiol and sectioned into 500 μm thick wafers using an Isomet® saw. Specimens were sterilized for 3 hours in 70% ethanol, subjected to a progressive wetting ladder, washed four times with PBS, and incubated overnight in MEM α supplemented with 40 w/v% FBS at 5% CO_2, 37°C. hMSCs were seeded at a density of 50,000 cells/cm^2 onto the polyHIPE sections. Viability at 24 hours, 72 hours, and 1 week was assessed utilizing the LIVE/DEAD assay kit (Molecular Probes). Cells were washed with PBS, stained with 2 μM calcein-AM (live) and 2 μM ethidium homodimer-1 (dead) for 30 minutes at 37°C, and washed with PBS for imaging. Imaging (3 images per specimen) was conducted on five specimens (n = 15) with a fluorescence microscope (Nikon Eclipse TE2000-S).

hMSC Proliferation on Thiol-Methacrylate PolyHIPEs

A Quant-iT™ PicoGreen® dsDNA Assay Kit (Molecular Probes) was utilized to quantify dsDNA to confirm thiol-methacrylate polyHIPEs supported hMSC proliferation. hMSCs were seeded at a density of 50,000 cells/cm^2 in standard growth media and allowed to adhere. After 24 hours, growth media or osteogenic media (growth media supplemented with 50 μg/mL ascorbic acid, 10 m*M* β-glycerophosphate, and 10 n*M* dexamethasone) was added and changed every 2 days for 10 additional days. PolyHIPE sections were removed from the culture wells and placed in unused wells for the lysis procedure prior to the PicoGreen assay to ensure only DNA from cells adhered to the scaffolds was measured. The assay was performed according to manufacturer instructions and fluorescence intensity was assessed using a plate reader (Tecan Infinite M200Pro) with excitation/emission wavelengths of 480/520 nm, respectively. Average cell number for day 1, 6, and 11 was determined by converting dsDNA values to individual cell number using 6.9 pg DNA/cell.[32] Specimens were analyzed in triplicate.

Alkaline Phosphatase Activity of hMSCs on Thiol-Methacrylate PolyHIPEs

Alkaline phosphatase activity of cells cultured on polyHIPE scaffolds was determined by monitoring the conversion of p-nitrophenyl phosphate (PNPP, Thermo Scientific) to p-nitrophenol. hMSCs were seeded at a density of 50,000 cells/cm^2 in standard growth media and allowed to adhere. After 24 hours, growth media or osteogenic media (growth media supplemented with 50 μg/mL ascorbic acid, 10 m*M* β-glycerophosphate, and 10 n*M* dexamethasone) was added and changed every 2 days for 10 additional days following measurement of ALP activity. Scaffold cultures were washed with ALP reaction buffer (100 mM Tris-HCl, pH 9, containing 100 mM KCl and 1 mM $MgCl^2$) and incubated with pNPP for 30 min. ALP activity was determined as the rate of PNPP conversion to p-nitrophenyl by measuring the absorbance at 405 nm (Tecan Infinite M200Pro) and normalized to cell number obtained from the PicoGreen assay. Specimens were analyzed in triplicate.

Author Manuscript Author Manuscript Author Manuscript Author Manuscript

Statistical Analysis

The data are displayed as mean ± standard deviation for each composition. A Student's t-test was performed to determine any statistically significant differences between compositions. All tests were carried out at a 95% confidence interval ($p<0.05$).

RESULTS AND DISCUSSION

Effect of Tetrathiol Concentration on PolyHIPE Fabrication and Architecture

Given that successful polyHIPE fabrication is dependent on characteristics such as macromer hydrophobicity and viscosity, the effect of the thiol additive on emulsion stability was first assessed. The octanol-water partition coefficient (logP) was used as a means of comparing molecular hydrophobicity.[33] LogP values are a measure of the differential solubility of a compound between two immiscible solvents, typically water and a hydrophobic solvent such as octanol. LogP values range from 0–20 where 0 corresponds to a hydrophilic molecule and 20 a hydrophobic molecule. The tetrathiol has a logP of 1.0 and a viscosity of 0.41 Pas compared to PFDMA with a logP of 3.4 and 0.13 Pas viscosity. Despite these differences in molecular hydrophobicity and viscosity, all compositions formed stable HIPEs and cured to rigid, interconnected monoliths. Pore size and homogeneity have been used as a relative measure of HIPE stability and strongly influence the monolith compressive properties and cellular behavior. The addition of the tetrathiol had a negligible effect on polyHIPE pore architecture, Figure 2. Likely, the low concentration of tetrathiol in the organic phase and rapid cure of the PFDMA HIPE limited time for phase separation and resulting effects on polyHIPE architecture. Retention of the desired pore architecture permits investigation of these polyHIPEs as scaffolds with reduced oxygen inhibition.

Effect of Tetrathiol Concentration on PolyHIPE Cure Rate

Developing a material with polymerization kinetics comparable to commonly utilized bone cements is critical to successful translation of our device. In general, the work time of dental cements is defined by ISO 9917 as the time at which a physician can manipulate and inject the graft without altering any material properties. The set time is the point at which the material has reached its gelation point and the network is set. According to ISO 5833, acrylic based cements should have a set time of 10–15 minutes. PolyHIPE cure rates were determined utilizing rheological methods with the onset and yielding of the storage modulus defined as the work and set times, respectively. PFDMA polyHIPE work and set times decreased with the addition of tetrathiol, Figure 3. The ~1.5 minute work time of PFDMA was reduced to 15 seconds with the addition of either 5 or 10 mol% tetrathiol. Similar trends were observed with the set time of these polyHIPEs. No significant difference in work and set times were observed between thiol concentrations utilizing this method. It was hypothesized that the extent of oxygen consumption needed prior to initiation provided the increased cure time of the PFDMA polyHIPE control. Increased induction time in the presence of inhibitory oxygen has been well documented in other vinyl mediated systems.[34] It has been reported that the equilibrium dissolved oxygen in acrylate systems is ~10^{-3} M.[20, 35] Decker et al. reported that the dissolved oxygen concentration in these systems must decrease by a factor of 300 to ~4×10^{-6} M prior to polymerization proceeding.[20] It was hypothesized that the addition of the thiol-based crosslinker permitted a reduced induction

Author Manuscript Author Manuscript Author Manuscript Author Manuscript

period and rapid network formation under ambient conditions due to the mixed mode chain and step growth polymerization mechanism of the thiol-methacrylate HIPEs. In addition to the increase in methacrylate polymerization rate with the addition of the thiol, the delay in methacrylate homopolymerization due to oxygen inhibition is minimized because the peroxy radicals can abstract the thiol hydrogen to generate thiyl radicals that can continue to propagate through addition or chain transfer.[36] Although the presented set times are approximately 10X faster than current bone cement standard values, the cure times can be modulated by decreasing redox initiator concentration, initiator and reducing agent ratios, and chemistries, as shown previously.[12]

Improved Resistance to Oxygen Inhibition in PolyHIPE Scaffolds

The inhibitory effect of molecular oxygen on the polymerization of multifunctional monomers has been widely acknowledged as a primary limitation in traditional free-radical polymerization.[34, 37–38] Several methods have been explored to overcome this limitation including the use of elevated concentrations of initiating agents, high-intensity irradiation sources, and fabrication within an inert environment.[39–40] However, less progress has been made in addressing this limitation in an injectable system intended for *in situ* polymerization. The primary aim of this work was to fabricate an injectable, polyHIPE bone graft that could provide more rapid and complete network formation in a clinically relevant environment. Specifically, we aimed to better understand the effect of oxygen inhibition on network formation in our polyHIPE system.

A major advantage of the emulsion templating platform is the ability to readily modulate pore architecture and surface area, properties vital to the success of tissue engineered scaffolds.[41] A range of surface areas have been reported from 3–20 m^2g^{-1} for traditional polyHIPEs to greater than 700 m^2g^{-1} for porogen modification scaffolds.[42–43] Although promising for promoting cell activity, the increased surface area of polyHIPEs provides a challenge over non-porous systems as it allows for increased diffusion of inhibitory oxygen into the HIPE surface. Near-complete network formation at these surfaces is critical to establishing suitable integration with native tissue and providing proper mechanical support. In order to better approximate monomer incorporation at the outer surface of the HIPE, network formation was first characterized in polyHIPEs cured in a high surface area morphology (flat bead) that maximized exposure to ambient oxygen. It was expected that the outer polyHIPE surface would be unable to compensate for the continual diffusion of oxygen into the sample and experience severely reduced polymerization and increased surface tackiness. Gel fraction was reduced to 38% in PFDMA control polyHIPEs cured under ambient conditions, Figure 4A. It follows that in the absence of inhibitory oxygen, monomer conversion in vinyl systems should increase to levels comparable to those of their oxygen resistant analogues. To this end, network formation was characterized in polyHIPEs cured under an inert nitrogen blanket in the high surface area morphology. PFDMA polyHIPE gel fraction increased to 60%, confirming the inhibitory effect of oxygen on our system. It is established that incorporation of thiol monomers mitigates the effects of oxygen exposure by acting as chain transfer agents and restoring initiating thiyl radicals. As expected, the addition of 5 and 10 mol% tetrathiol improved network formation to greater than 60% and 70% when cured under ambient conditions. It was hypothesized that the

Author Manuscript Author Manuscript Author Manuscript Author Manuscript

increase in continuous phase viscosity provided by tetrathiol addition further served to improve inhibition resistance by decreasing oxygen diffusion into the scaffold. The effect of monomer viscosity in reducing oxygen inhibition has been studied in other thiol-acrylate systems.[25, 44] Furthermore, network formation in thiol-methacrylate polyHIPEs increased to a lesser extent when cured under inert conditions as compared to PFDMA polyHIPE controls. Differences in network formation between methacrylate and thiol-methacrylate scaffolds cured under nitrogen-purged conditions was attributed to the presence of small amounts of residual oxygen.

Oxygen inhibition has also been modeled in acrylate systems to identify the effect of film thickness on oxygen inhibition.[24] It is accepted that as film thickness increases, inhibitory oxygen levels decrease and allow for polymerization. The subsequent increase in viscosity during cure serves to limit subsequent diffusion of oxygen. Therefore, it was expected that network formation of PFDMA monomers in bulk-cured scaffolds would be comparable to thiol-methacrylate systems. Gel fraction values were 85% for PFDMA controls, 87% for 5 mol% tetrathiol, and 92% for 10 mol% tetrathiol, Figure 4B. Observed increases in gel fraction for thiol-methacrylate polyHIPEs under these conditions was attributed to the presence of dissolved oxygen prior to cure. Previous work has demonstrated injectable, fumarate based systems with sol fraction values greater than 10% to be biocompatible and support new bone formation *in vitro* and *in vivo*.[45–47] Furthermore, commercially available bone cements have been shown to exhibit site specific network formation within the implant site.[48] Our ability to improve network formation in the presence of oxygen, combined with the success of similar fumarate systems, illustrates the strong clinical potential of these polyHIPE bone grafts.

Improved Storage Stability with Hydroquinone Additive

We have previously demonstrated that redox initiated polyHIPEs have the ability to be stored for extended periods and serve as an off-the-shelf graft. Although thiol-methacrylate polyHIPEs demonstrated improved resistance to oxygen inhibition, an increase in emulsion viscosity that precluded proper injection and space filling was observed after only one week of storage. It has been reported that thiol monomers may act as a primary reducing agent and yield high monomer conversion rates in redox initiated thiol-ene systems.[49] It was hypothesized that the loss of storage stability in our system resulted from the uninhibited reaction of benzoyl peroxide with the tetrathiol monomer during fabrication and storage. This allowed marginal levels of initiating radicals to form prior to mixing, facilitate early crosslinking, and increase emulsion viscosity. This high reactivity of thiol-ene systems often prompts the need for additional stabilizing agents to prevent undesired polymerization.[22, 50] To this end, hydroquinone was added as a stabilizing agent to the HIPE to scavenge propagating radicals and prevent early polymerization, Figure 5A. Quinone based inhibitors have been utilized to control the induction period and polymerization rate of thiol-ene polymerizations initiated with benzoyl peroxide.[49] Inhibitor concentration of 200 PPM was selected as the lowest concentration required to prevent early polymerization while retaining a reduced activation profile to allow rapid cure during redox initiation. Storage time of stabilized polyHIPEs with 10 mol% tetrathiol was monitored for 30 days to ensure an increase in storage time. Cure rate and gel fraction of stabilzed polyHIPEs was characterized

Author Manuscript Author Manuscript Author Manuscript Author Manuscript

to ensure the addition of inhibitor did not negatively impact key scaffold properties. Although a minimal decrease in cure rate and gel fraction was observed in stabilized polyHIPEs as compared to non-stabilized controls, the values still provide a marked increase over PFDMA only and support significant resistance to oxygen inhibition, Figure 5.

Retention of Compressive Properties

PFDMA/tetrathiol polyHIPE compressive modulus and yield strength were assessed to ensure that these polyHIPEs retained appropriate compressive mechanical properties for use as bone grafting materials. A significant decrease in compressive modulus and yield strength was observed with an increase in tetrathiol concentration, Figure 6. PFDMA polyHIPEs fabricated with greater than 10 mol% tetrathiol exhibited decreases in compressive properties greater than 40% as compared to PFDMA controls and were not further characterized. PFDMA polyHIPEs with 10 mol% tetrathiol resulted in an average compressive modulus of 15 MPa and strength of 0.7 MPa. It was hypothesized that the observed decrease in compressive properties was due to a reduction in crosslink density. Increasing the number of thiol functional groups resulted in an increase in chain transfer during polymerization with a resulting reduction in chain length and the number of crosslinks attached to each kinetic chain. A similar decrease in compressive modulus with increasing amount of trithiol was observed by Rydholm et al. in poly(ethylene glycol)-based hydrogels.[36]

Although there was a reduction in compressive modulus and yield strength, the values were still within the range of typical bone grafting materials. The ability to promote new bone formation within porous and biodegradable systems has been reported with scaffold compressive moduli ranging from 2–100 MPa.[51–54] Introduction of porosity into these systems is often achieved through particulate leaching or gas foaming, techniques that may result in reduced compressive properties as porosity is increased.[55–58] In contrast, emulsion templating yields a uniform and spherical pore architecture that eliminates the potential for stress concentrators. As a result, PFDMA and thiol-methacrylate polyHIPEs exhibit improved mechanical properties over similar systems of >70% porosity, and retain compressive properties within a range demonstrated suitable *in vivo*.[55–56] Recent work has focused on incorporating additional methacrylate-functionalized monomers into the HIPE organic phase to further modulate viscosity for cell encapsulation. PolyHIPEs fabricated from these monomers alone have increased crosslink density and therefore increased compressive properties. As a result, it is probable that modulating the molar ratio of PFDMA:methacrylated-monomer will result in an increase in compressive properties relative to standard PFDMA polyHIPEs.

Tunable Degradation Profiles

An additional goal of fabricating thiol-methacrylate polyHIPEs was to generate scaffolds with a tunable degradation profile for future matching with *in vivo* neotissue formation. Thiol-methacrylate scaffolds with tunable degradation profiles have previously shown promise for use as tissue engineered scaffolds. Accelerated degradation scouting studies were conducted at two sodium hydroxide concentrations (0.25 and 0.5 M NaOH) to determine the effect of tetrathiol on PFDMA polyHIPE degradation. Values reported reflect

Author Manuscript Author Manuscript Author Manuscript Author Manuscript

mass loss after accounting for the theoretical mass of the surfactant, PGPR. An increase in mass loss was observed with an increase in tetrathiol concentration when assessed in basic, accelerated conditions, Figure 7. In 0.5 M NaOH conditions, all thiol-methacrylate polyHIPEs exhibited complete loss of integrity by 3 weeks whereas the PFDMA polyHIPE control maintained ~35% mass loss after the initial mass loss at 1 week. The initial PFDMA mass loss at one week was attributed to the removal of unreacted macromer or the formation of rapidly degrading microgels, which was further supported with the lower gel fraction of PFDMA control polyHIPEs.[59] This increase in hydrolytic degradation rate of thiol-methacrylate polyHIPEs was attributed to the incorporation of β-thioesters and reduction in crosslink density due to increased chain transfer.[60] Schoenmaker et al. demonstrated an increase in atomic charge on the carbon atom of an ester as the distance from the sulfide decreased rendering it more susceptible to hydrolytic attack. It is believed that the increased number of hydrolytically labile ester linkages present in the fumarate backbone of PFDMA would allow for increased degradation over similar methacrylate monomers without requiring increased thiol content. Although an increase in degradation rate was observed *in vitro*, the *in vivo* degradation rate of these specific polyHIPE formulations is unknown and would need to be explored in an animal model. Degradation and cytocompatibility profiles of similar fumarate based systems have been previously reported in *in vitro* and *in vivo* models.[61–63]

Osteogenic Activity Supported on Thiol-Methacrylate PolyHIPEs

A primary aim in bone tissue engineering is the development of scaffolds that allow for the recruitment and retention of stem cell populations at the site of injury. Therefore, a main goal of this work was to create a highly porous, oxygen resistant bone graft that would support desired cellular activity through verification of viability, proliferation and osteogenic activity of hMSCs. Studies with poly(propylene fumarate)-based biomaterial scaffolds with similar chemistries demonstrated *in vitro* cytocompatibility and *in vivo* biocompatibility illustrating the potential of PFDMA based systems.[51, 64–65] Furthermore, our lab previously demonstrated PFDMA polyHIPEs are capable of supporting hMSC viability up to 2 weeks.[12] Given the proposed application of polyHIPEs to be injected and cured *in situ*, an extraction study was performed on cross-linked PFDMA control and 10 mol% thiol-methacrylate scaffolds to provide an initial assessment of the cytocompatibility of the injectable polyHIPE immediately following cure. Although acute viability of hMSCs exposed to undiluted extraction media of polyHIPE bead specimens was poor (<30%), a significant improvement in acute viability and morphology was observed for the thiol-methacrylate polyHIPEs at 0.5 vol% over the PFDMA control. Viability increased to greater than 94%, with no morphological differences observed between hMSCs cultured with the thiol-methacrylate extract compared to standard growth media, Figure 8. The bead morphology was used to provide high surface-area-to-volume ratios that would maximize the effect of oxygen inhibition and sol fraction. The 2X dilution of the extraction solution was used to estimate extractable concentrations of bulk polymerized specimens (roughly 50% sol fraction of bead specimens, Figure 4), which are expected to be more similar to bone grafting applications. It was hypothesized that the improvement in network formation in thiol-methacrylate systems reduced leachable monomer content present in the extraction media and resulted in improved viability over the PFDMA control. Supplementary Figure S2

Author Manuscript Author Manuscript Author Manuscript Author Manuscript

illustrates a decrease in PFDMA macromer content present in extraction media as determined by ^{1}H NMR.

After confirming an improvement in acute cytocompatibility with tetrathiol incorporation, hMSCs were seeded directly onto cleaned PFDMA control and 10 mol% thiol-methacrylate polyHIPEs up to one week to further characterize cell response. Thiol-methacrylate polyHIPE scaffolds supported hMSC viability of greater than 80%, while PFDMA controls exhibited viability greater than 90% Figure 9. Minor differences in viability between scaffold compositions was attributed to differences in initial cell attachment as a result of altered surface chemistry and protein adsorption. In addition, a 2 and 3 fold increase in cell number was observed at 11 days on PFDMA controls and thiol-methacrylate polyHIPEs respectively, Figure 10. The ability of thiol-methacrylate polyHIPEs to support long-term proliferation permits further investigation into osteogenic activity of seeded hMSCs. Notably, the specimens were sterilized with ethanol washes prior to cell seeding that may remove extractables and not fully replicate the injected form, which is a limitation of the current study. In future studies, each of the components will be sterilized prior to HIPE formation and sterility maintained prior to injection. This method will permit cytocompatibility and other biocompatibility assessments immediately following injection and cure without additional processing. It is expected that possible leachables will likely to be removed by the native vasculature, as postulated previously for other fumarate systems.[45]

The ability to direct bone-marrow derived cells down a discrete lineage is a potent tool for improving the regenerative capacity of our tissue engineered graft. We previously demonstrated the ability of polyHIPE scaffolds to serve as a delivery vehicle for a multitude of osteoinductive agents and support osteogenic activity of seeded hMSCs as confirmed by early and late stage gene expression.[13] Furthermore, unmodified PFDMA scaffolds also reported osteogenic differentiation under standard culture conditions demonstrating an inherent osteoinductive character of these grafts. In this study, ALP enzyme activity was assessed as an early marker of osteoblastic differentiation of seeded hMSCs to confirm that thiol-methacrylate polyHIPEs retained this ability to support osteogenic activity. ALP activity increased (2–3 fold) for all scaffold compositions at 11 days for scaffolds cultured in both growth and osteogenic media, Figure 11. It was noted that the rate of proliferation decreased while the rate of increase in ALP activity increased for both scaffold compositions from day 6 to day 11, when hMSCs were cultured in ostegenic media. No significant differences were observed between PFDMA control and thiol-methacrylate polyHIPEs. These observations support established activity profiles for MSC differentiation and illustrate the retained ability of these grafts to support osteogenic activity.

Although initial activity of MSCs seeded on our polyHIPE graft provide a clear promise for success *in vitro*, a future goal of this project is the development of an injectable polyHIPE system with the potential to support encapsulation and *in vivo* delivery of these cells to the injury site. The addition of tetrathiol into our injectable polyHIPE may provide added benefit in this work to adapt our system as a rigid cell carrier. Roberts et al. demonstrated that thiol-ene based polymerization mechanisms can have long-term effects on the quality of engineered cartilage in thiol-ene systems over acrylate based PEG hydrogel scaffolds.[66] Furthermore, the role of thiol-ene chemistries in reducing intracellular ROS damage was

Author Manuscript Author Manuscript Author Manuscript Author Manuscript

noted, a characteristic of thiol-methacrylate polyHIPEs that would further support viability and retention of encapsulated cells.

CONCLUSIONS

This study demonstrates the potential of thiol-methacrylate polyHIPEs to serve as an injectable bone graft with improved resistance to oxygen inhibition. Incorporation of tetrathiol monomer provided more rapid and complete network formation in the presence of oxygen with minimal impact on compressive modulus, yield strength, and pore architecture. The introduction of β-thioesters also served to increase the rate of hydrolytic degradation of the polyHIPE, providing a potent tool for tuning desired degradation profiles. Finally, thiol-methacrylate polyHIPEs demonstrated strong potential as a tissue engineered scaffold by supporting extended viability and proliferation of hMSCs and retaining the osteoconductive character previously observed in our PFDMA system. Overall, the investigation of thiol-methacrylate based grafts improves the translational potential of polyHIPEs by providing a material with improved function in clinically relevant environments and demonstrating the potential to influence cellular activity.

Acknowledgments

Funding was provided by NIH R21 EB016393. The authors acknowledge Palsgaard USA for providing PGPR 4125. Human mesenchymal stem cells were provided by the Texas A&M Health Science Center College of Medicine Institute for Regenerative Medicine at Scott & White through a grant from NCRR of the NIH, Grant # P40RR017447.

References

1. Middleton JC, Tipton AJ. Synthetic biodegradable polymers as orthopedic devices. Biomaterials. 2000; 21(23):2335–2346. [PubMed: 11055281]
2. Hacker M, Ringhofer M, Appel B, Neubauer M, Vogel T, Young S, Mikos AG, Blunk T, Göpferich A, Schulz MB. Solid lipid templating of macroporous tissue engineering scaffolds. Biomaterials. 2007; 28(24):3497–3507. [PubMed: 17482257]
3. Harris LD, Kim B-S, Mooney DJ. Open pore biodegradable matrices formed with gas foaming. Journal of biomedical materials research. 1998; 42(3):396–402. [PubMed: 9788501]
4. Karageorgiou V, Kaplan D. Porosity of 3D biomaterial scaffolds and osteogenesis. Biomaterials. 2005; 26(27):5474–5491. [PubMed: 15860204]
5. Kim TK, Yoon JJ, Lee DS, Park TG. Gas foamed open porous biodegradable polymeric microspheres. Biomaterials. 2006; 27(2):152–159. [PubMed: 16023197]
6. Mistry AS, Cheng SH, Yeh T, Christenson E, Jansen JA, Mikos AG. Fabrication and in vitro degradation of porous fumarate based polymer/alumoxane nanocomposite scaffolds for bone tissue engineering. Journal of Biomedical Materials Research Part A. 2009; 89(1):68–79. [PubMed: 18428800]
7. Pham QP, Sharma U, Mikos AG. Electrospinning of polymeric nanofibers for tissue engineering applications: a review. Tissue engineering. 2006; 12(5):1197–1211. [PubMed: 16771634]
8. Rose FR, Oreffo RO. Bone tissue engineering: hope vs hype. Biochemical and biophysical research communications. 2002; 292(1):1–7. [PubMed: 11890663]
9. Akay G, Birch MA, Bokhari MA. Microcellular polyHIPE polymer supports osteoblast growth and bone formation in vitro. Biomaterials. 2004; 25:3991–4000. [PubMed: 15046889]
10. Moglia RS, Holm JL, Sears NA, Wilson CJ, Harrison DM, Cosgriff-Hernandez E. Injectable PolyHIPEs as High-Porosity Bone Grafts. Biomacromolecules. 2011; 12(10):3621–3628. DOI: 10.1021/bm2008839 [PubMed: 21861465]

Author Manuscript Author Manuscript Author Manuscript Author Manuscript

11. Moglia RS, Robinson JL, Muschenborn AD, Touchet TJ, Maitland DJ, Cosgriff-Hernandez E. Injectable polyMIPE scaffolds for soft tissue regeneration. Polymer. 2014; 55(1):426–434.
12. Moglia RS, Whitely M, Dhavalikar P, Robinson J, Pearce H, Brooks M, Stuebben M, Cordner N, Cosgriff-Hernandez E. Injectable Polymerized High Internal Phase Emulsions with Rapid in Situ Curing. Biomacromolecules. 2014; 15(8):2870–2878. DOI: 10.1021/bm500754r [PubMed: 25006990]
13. Robinson JL, McEnery MA, Pearce H, Whitely ME, Munoz-Pinto DJ, Hahn MS, Li H, Sears NA, Cosgriff-Hernandez E. Osteoinductive PolyHIPE Foams as Injectable Bone Grafts. Tissue Engineering Part A. 2016; 22(5–6):403–414. [PubMed: 26739120]
14. Robinson JL, Moglia RS, Stuebben MC, McEnery MA, Cosgriff-Hernandez E. Achieving interconnected pore architecture in injectable polyHIPEs for bone tissue engineering. Tissue Engineering Part A. 2014; 20(5–6):1103–1112. [PubMed: 24124758]
15. Barbetta A, Dentini M, Zannoni EM, De Stefano ME. Tailoring the Porosity and Morphology of Gelatin-Methacrylate PolyHIPE Scaffolds for Tissue Engineering Applications. Langmuir. 2005; 21(26):12333–12341. [PubMed: 16343011]
16. Busby W, Cameron NR, Jahoda CAB. Emulsion-derived foams (polyHIPEs) containing poly(ε-caprolactone) as matrixes for tissue engineering. Biomacromolecules. 2001; 2(1):154–164. [PubMed: 11749167]
17. Hayman MW, Smith KH, Cameron NR, Przyborskia SA. Growth of human stem cell-derived neurons on solid three-dimensional polymers. J Biochem Biophys Methods. 2005; 62:231–240. [PubMed: 15733583]
18. Peter SJ, Miller MJ, Yasko AW, Yaszemski MJ, Mikos AG. Polymer concepts in tissue engineering. Journal of Biomedical Materials Research. 1998; 43(4):422–427. DOI: 10.1002/(SICI)1097-4636(199824)43:4<422::AID-JBM9>3.0.CO;2-1 [PubMed: 9855200]
19. Decker C. Effect of UV radiation on polymers. Marcel Dekker, Handbook of Polymer Science and Technology. 1989; 3:541–608.
20. Decker C, Jenkins AD. Kinetic approach of oxygen inhibition in ultraviolet- and laser-induced polymerizations. Macromolecules. 1985; 18(6):1241–1244. DOI: 10.1021/ma00148a034
21. Rueggeberg F, Margeson D. The effect of oxygen inhibition on an unfilled/filled composite system. Journal of Dental Research. 1990; 69(10):1652–1658. [PubMed: 2212209]
22. Cramer NB, Bowman CN. Kinetics of thiol-ene and thiol–acrylate photopolymerizations with real–time fourier transform infrared. Journal of Polymer Science Part A: Polymer Chemistry. 2001; 39(19):3311–3319. DOI: 10.1002/pola.1314
23. Morgan CR, Magnotta F, Ketley AD. Thiol/ene photocurable polymers. Journal of Polymer Science: Polymer Chemistry Edition. 1977; 15(3):627–645. DOI: 10.1002/pol.1977.170150311
24. O'Brien AK, Bowman CN. Modeling the effect of oxygen on photopolymerization kinetics. Macromolecular Theory and Simulations. 2006; 15(2):176–182.
25. O'Brien AK, Cramer NB, Bowman CN. Oxygen inhibition in thiol-acrylate photopolymerizations. Journal of Polymer Science Part A: Polymer Chemistry. 2006; 44(6):2007–2014. DOI: 10.1002/pola.21304
26. Caldwell S, Johnson DW, Didsbury MP, Murray BA, Wu JJ, Przyborski SA, Cameron NR. Degradable emulsion-templated scaffolds for tissue engineering from thiol-ene photopolymerisation. Soft Matter. 2012; 8(40):10344–10351.
27. Lovelady E, Kimmins SD, Wu J, Cameron NR. Preparation of emulsion-templated porous polymers using thiol-ene and thiol-yne chemistry. Polym Chem. 2011; 2(3):559–562. DOI: 10.1039/c0py00374c
28. Langford C, Johnson D, Cameron N. Chemical functionalization of emulsion-templated porous polymers by thiol-ene "click" chemistry. Polymer Chemistry. 2014; 5(21):6200–6206.
29. Timmer MD, Horch AR, Ambrose CG, Mikos AG. Effect of physiological temperature on the mechanical properties and network structure of biodegradable poly(propylene fumarate)-based networks. J Biomat Sci Polym Ed. 2003; 14(4):369–382.
30. Foudazi R, Gokun P, Feke DL, Rowan SJ, Manas-Zloczower I. Chemorheology of Poly(high internal phase emulsions). Macromolecules. 2013; 46(13):5393–5396. DOI: 10.1021/ma401157b

Author Manuscript Author Manuscript Author Manuscript Author Manuscript

31. Barbetta A, Cameron NR. Morphology and surface area of emulsion-derived (PolyHIPE) solid foams prepared with oil-phase soluble porogenic solvents: Span 80 as surfactant. Macromolecules. 2004; 37(9):3188–3201.
32. Gregory TR. Nucleotypic effects without nuclei: genome size and erythrocyte size in mammals. Genome. 2000; 43(5):895–901. [PubMed: 11081981]
33. http://www.molinspiration.com/
34. Kloosterboer, JG. Electronic applications. Springer; 1988. Network formation by chain crosslinking photopolymerization and its applications in electronics; p. 1-61.
35. Gou L, Coretsopoulos CN, Scranton AB. Measurement of the dissolved oxygen concentration in acrylate monomers with a novel photochemical method. Journal of Polymer Science Part A: Polymer Chemistry. 2004; 42(5):1285–1292.
36. Rydholm AE, Bowman CN, Anseth KS. Degradable thiol-acrylate photopolymers: polymerization and degradation behavior of an in situ forming biomaterial. Biomaterials. 2005; 26(22):4495–4506. [PubMed: 15722118]
37. Bowman CN, Kloxin CJ. Toward an enhanced understanding and implementation of photopolymerization reactions. AIChE Journal. 2008; 54(11):2775–2795.
38. Decker C. UV-curing chemistry: past, present, and future. JCT, Journal of coatings technology. 1987; 59(751):97–106.
39. Studer K, Decker C, Beck E, Schwalm R. Overcoming oxygen inhibition in UV-curing of acrylate coatings by carbon dioxide inerting, Part I. Progress in Organic Coatings. 2003; 48(1):92–100.
40. Ligon SC, Husár B, Wutzel H, Holman R, Liska R. Strategies to reduce oxygen inhibition in photoinduced polymerization. Chemical reviews. 2013; 114(1):557–589. [PubMed: 24083614]
41. Murphy CM, Haugh MG, O'Brien FJ. The effect of mean pore size on cell attachment, proliferation and migration in collagen–glycosaminoglycan scaffolds for bone tissue engineering. Biomaterials. 2010; 31(3):461–466. [PubMed: 19819008]
42. Barbetta, A., Carnachan, RJ., Smith, KH., Zhao, Ct, Cameron, NR., Kataky, R., Hayman, M., Przyborski, SA., Swan, M. Porous polymers by emulsion templating. Macromolecular Symposia, Wiley Online Library; 2005. p. 203-212.
43. Hainey P, Huxham I, Rowatt B, Sherrington D, Tetley L. Synthesis and ultrastructural studies of styrene-divinylbenzene polyhipe polymers. Macromolecules. 1991; 24(1):117–121.
44. Lee T, Guymon C, Jönsson ES, Hoyle C. The effect of monomer structure on oxygen inhibition of (meth) acrylates photopolymerization. Polymer. 2004; 45(18):6155–6162.
45. Peter SJ, Lu L, Kim DJ, Mikos AG. Marrow stromal osteoblast function on a poly (propylene fumarate)/β-tricalcium phosphate biodegradable orthopaedic composite. Biomaterials. 2000; 21(12):1207–1213. [PubMed: 10811302]
46. Peter SJ, Nolley JA, Widmer MS, Merwin JE, Yaszemski MJ, Yasko AW, Engel PS, Mikos AG. In vitro degradation of a poly (propylene fumarate)/β-tricalcium phosphate composite orthopaedic scaffold. Tissue Engineering. 1997; 3(2):207–215.
47. Yaszemski MJ, Payne RG, Hayes WC, Langer RS, Aufdemorte TB, Mikos AG. The ingrowth of new bone tissue and initial mechanical properties of a degrading polymeric composite scaffold. Tissue engineering. 1995; 1(1):41–52. [PubMed: 19877914]
48. Stańczyk M, Van Rietbergen B. Thermal analysis of bone cement polymerisation at the cement–bone interface. Journal of biomechanics. 2004; 37(12):1803–1810. [PubMed: 15519587]
49. Cole MA, Jankousky KC, Bowman CN. Redox initiation of bulk thiol-ene polymerizations. Polymer chemistry. 2013; 4(4):1167–1175. [PubMed: 23565125]
50. Fouassier, J-P., Rabek, JF. Radiation curing in polymer science and technology: Practical aspects and applications. Vol. 4. Springer Science & Business Media; 1993.
51. Mistry A, Pham Q, Schouten C, Yeh T, Christensen E, Mikos A, Jansen J. *In vivo* bone biocompatibility and degradation of porous fumarate-based polymer/alumoxane nanocomposites for bone tissue engineering. J Biomed Mater Res A. 2010; 92A(2):451–462.
52. Patel ZS, Young S, Tabata Y, Jansen JA, Wong ME, Mikos AG. Dual delivery of an angiogenic and an osteogenic growth factor for bone regeneration in a critical size defect model. Bone. 2008; 43(5):931–940. [PubMed: 18675385]

Author Manuscript Author Manuscript Author Manuscript Author Manuscript

53. Kim S-S, Park MS, Jeon O, Choi CY, Kim B-S. Poly (lactide-co-glycolide)/hydroxyapatite composite scaffolds for bone tissue engineering. Biomaterials. 2006; 27(8):1399–1409. [PubMed: 16169074]
54. Dumas JE, BrownBaer PB, Prieto EM, Guda T, Hale RG, Wenke JC, Guelcher SA. Injectable reactive biocomposites for bone healing in critical-size rabbit calvarial defects. Biomedical Materials. 2012; 7(2):024112. [PubMed: 22456057]
55. Kim CW, Talac R, Lu L, Moore MJ, Currier BL, Yaszemski MJ. Characterization of porous injectable poly (propylene fumarate) based bone graft substitute. Journal of Biomedical Materials Research Part A. 2008; 85(4):1114–1119. [PubMed: 17941027]
56. Fisher PJ, Holland TA, Dean D, Engel PS, Mikos AG. Synthesis and properties of photocross-linked poly (propylene fumarate) scaffolds. Journal of Biomaterials Science, Polymer Edition. 2001; 12(6):673–687. [PubMed: 11556743]
57. Dumas JE, Zienkiewicz K, Tanner SA, Prieto EM, Bhattacharyya S, Guelcher SA. Synthesis and characterization of an injectable allograft bone/polymer composite bone void filler with tunable mechanical properties. Tissue Engineering Part A. 2010; 16(8):2505–2518. [PubMed: 20218874]
58. Gorna K, Gogolewski S. Biodegradable porous polyurethane scaffolds for tissue repair and regeneration. Journal of Biomedical Materials Research Part A. 2006; 79(1):128–138. [PubMed: 16779769]
59. Graham NB, Cameron A. Nanogels and microgels: The new polymeric materials playground. Pure Appl Chem. 1998; 70(6):1271–1275. DOI: 10.1351/pac199870061271
60. Schoenmakers RG, van de Wetering P, Elbert DL, Hubbell JA. The effect of the linker on the hydrolysis rate of drug-linked ester bonds. J Control Release. 2004; 95(2):291–300. [PubMed: 14980777]
61. Timmer MD, Shin H, Horch RA, Ambrose CG, Mikos AG. In vitro cytotoxicity of injectable and biodegradable poly (propylene fumarate)-based networks: unreacted macromers, cross-linked networks, and degradation products. Biomacromolecules. 2003; 4(4):1026–1033. [PubMed: 12857088]
62. Peter SJ, Miller ST, Zhu G, Yasko AW, Mikos AG. In vivo degradation of a poly(propylene fumarate)/β-tricalcium phosphate injectable composite scaffold. J Biomed Mater Res. 1998; 41(1): 1–7. DOI: 10.1002/(SICI)1097-4636(199807)41:1<1::AID-JBM1>3.0.CO;2-N [PubMed: 9641618]
63. He S, Timmer M, Yaszemski MJ, Yasko A, Engel P, Mikos A. Synthesis of biodegradable poly (propylene fumarate) networks with poly (propylene fumarate)-diacrylate macromers as crosslinking agents and characterization of their degradation products. Polymer. 2001; 42(3):1251–1260.
64. Mistry AS, Cheng SH, Yeh T, Christenson E, Jansen JA, Mikos AG. Fabrication and in vitro degradation of porous fumarate-based polymer/alumoxane nanocomposite scaffolds for bone tissue engineering. J Biomed Mater Res A. 2009; 89A(1):68–79.
65. Shi, Xea. Fabrication of porous ultra-short single-walled carbon nanotube nanocomposite scaffolds for bone tissue engineering. Biomaterials. 2007; 28(28):4078–4090. DOI: 10.1016/j.biomaterials.2007.05.033 [PubMed: 17576009]
66. Roberts JJ, Bryant SJ. Comparison of photopolymerizable thiol-ene PEG and acrylate-based PEG hydrogels for cartilage development. Biomaterials. 2013; 34(38):9969–9979. [PubMed: 24060418]

Author Manuscript Author Manuscript Author Manuscript Author Manuscript

A) Propylene Fumarate Dimethacrylate *(PFDMA)*

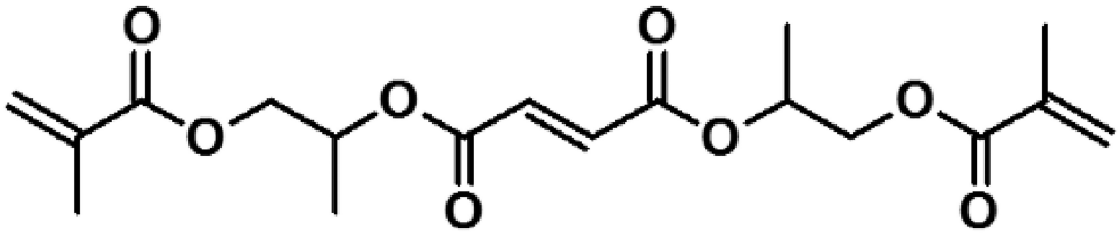

B) Pentaerythritol tetrakis (3-mercaptoproprionate) *(tetrathiol)*

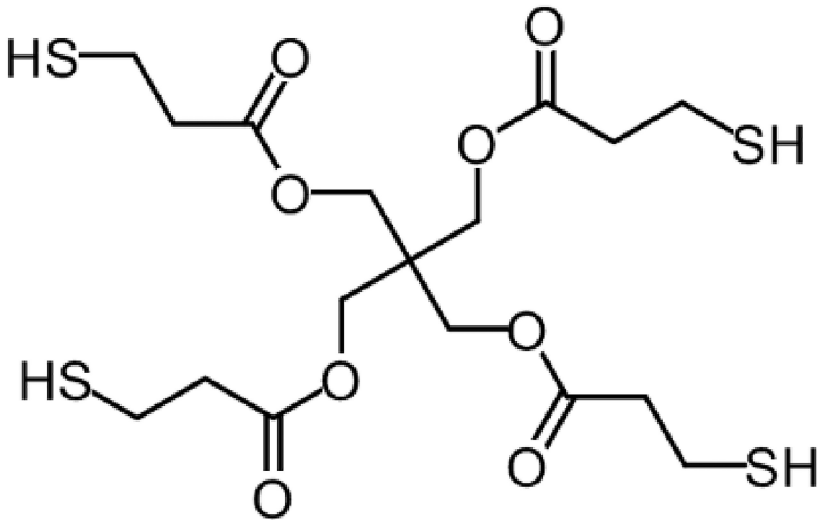

Figure 1.
Molecular structure of propylene fumarate dimethacrylate (PFDMA) (A) and pentaerythritol tetrakis(3-mercaptoproprionate) (tetrathiol) (B).

Author Manuscript
Author Manuscript
Author Manuscript
Author Manuscript

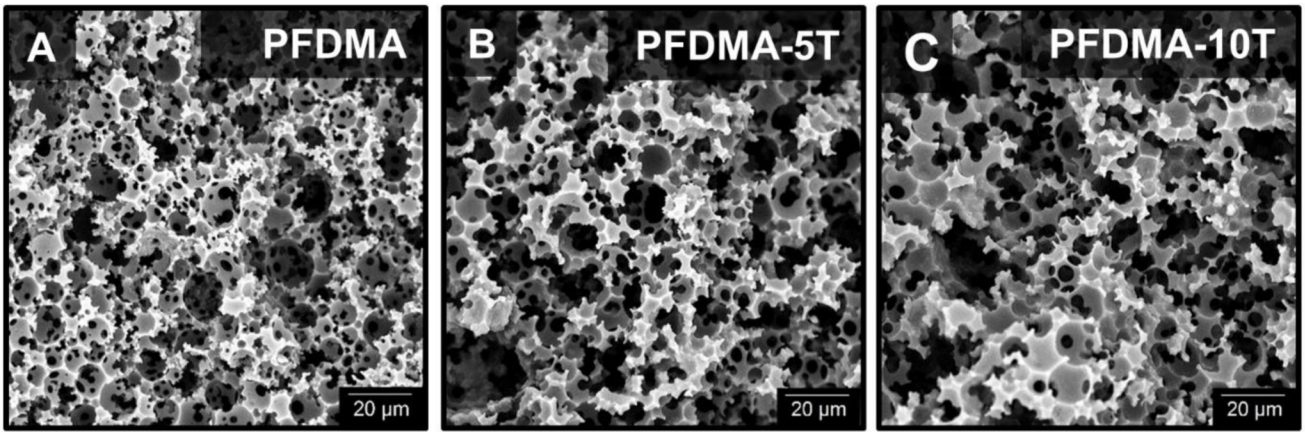

Figure 2.

Representative scanning electron microscopy (SEM) micrographs of PFDMA (A), PFDMA-5T (B), and PFDMA-10T (C) polyHIPE pore architecture.

Author Manuscript Author Manuscript Author Manuscript Author Manuscript

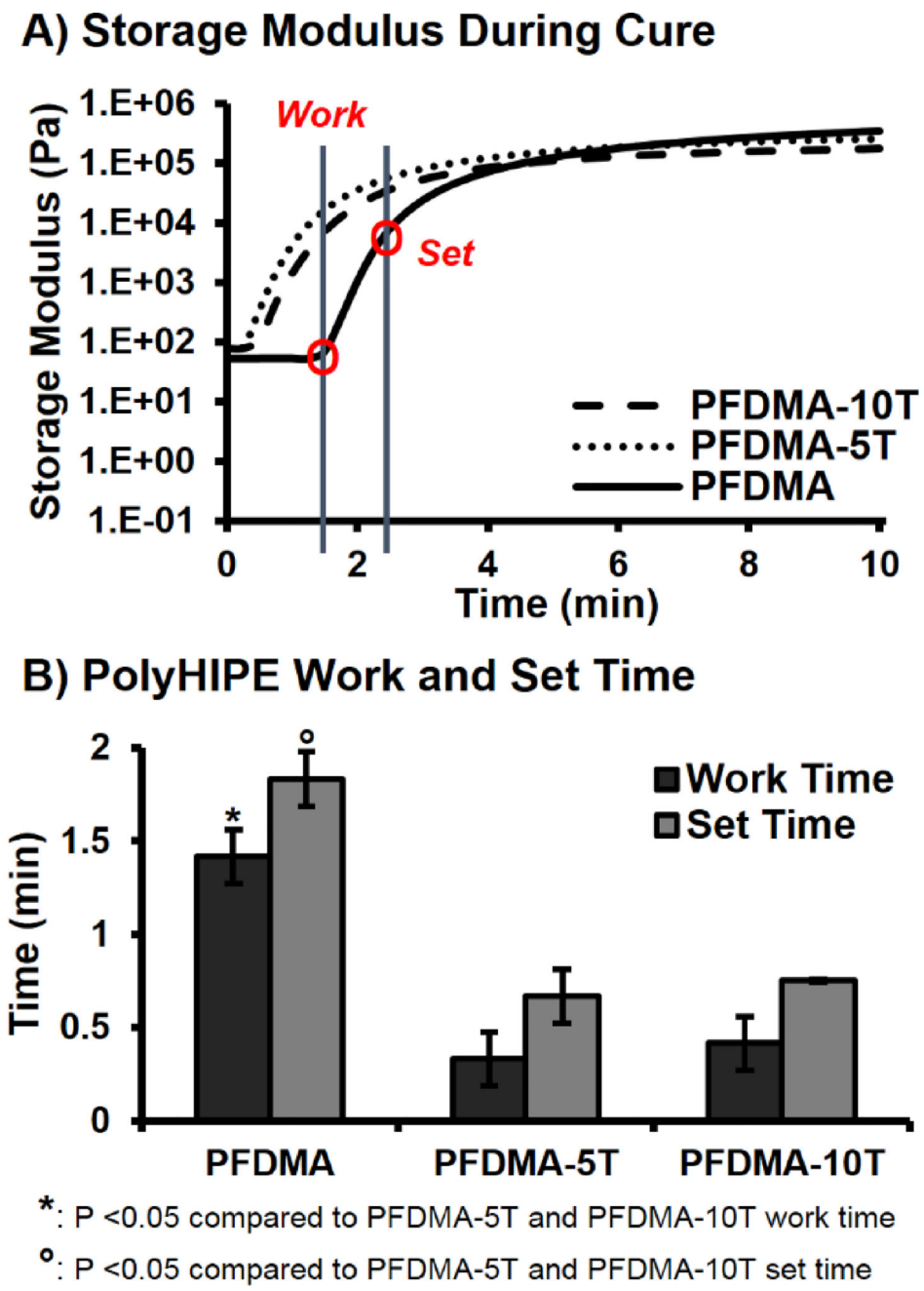

Figure 3.

Storage modulus during polymerization of polyHIPE (A) and work and set times (B) of polyHIPEs cured at 37 °C with 1.0 wt% initiator and reducing agent.

Author Manuscript Author Manuscript Author Manuscript Author Manuscript

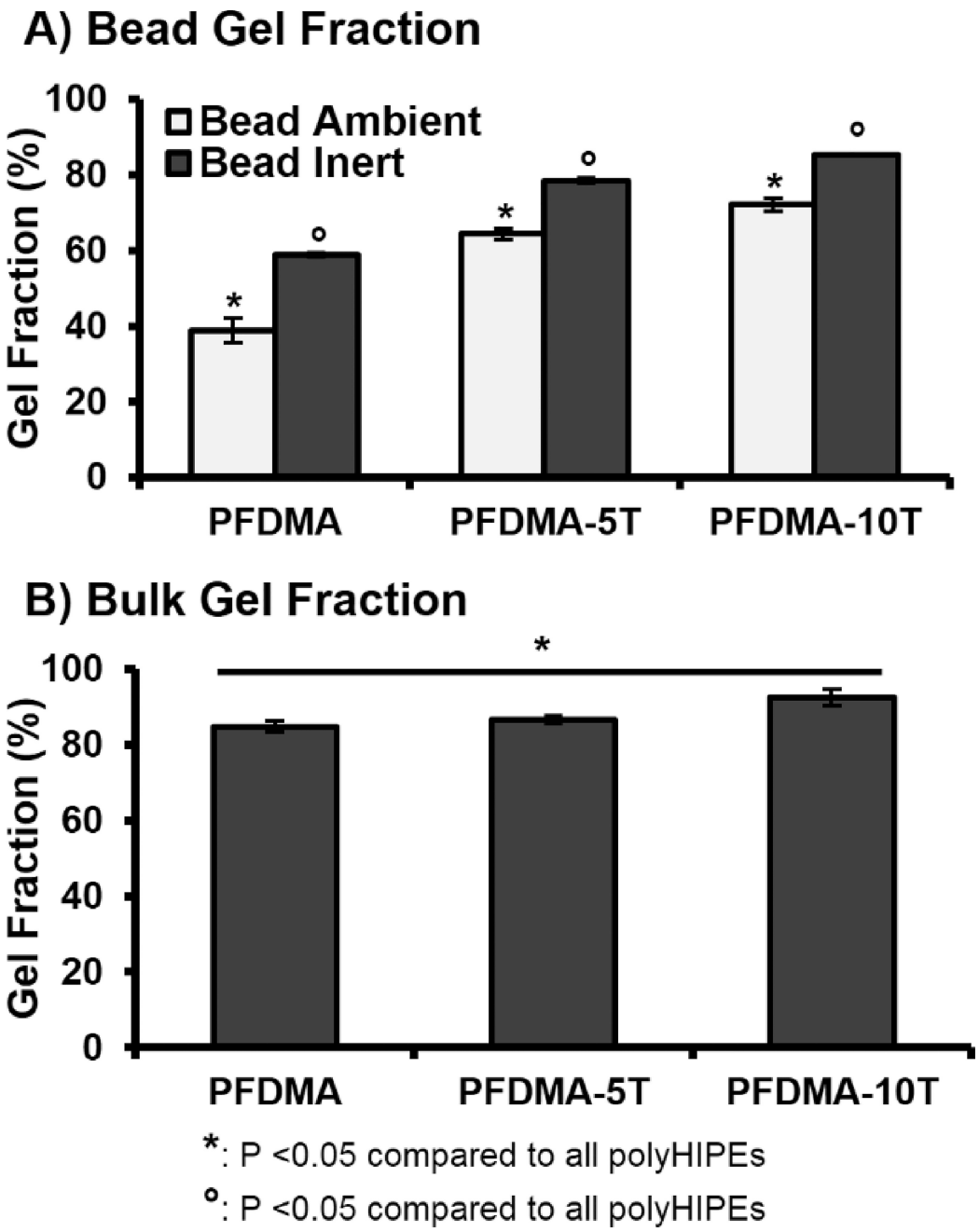

Figure 4.

The effect of increasing tetrathiol concentration on average gel fraction for high surface-area-to-volume ratio polyHIPEs cured under ambient and low oxygen conditions (A) and bulk cured polyHIPEs cured under ambient conditions (B).

Author Manuscript Author Manuscript Author Manuscript Author Manuscript

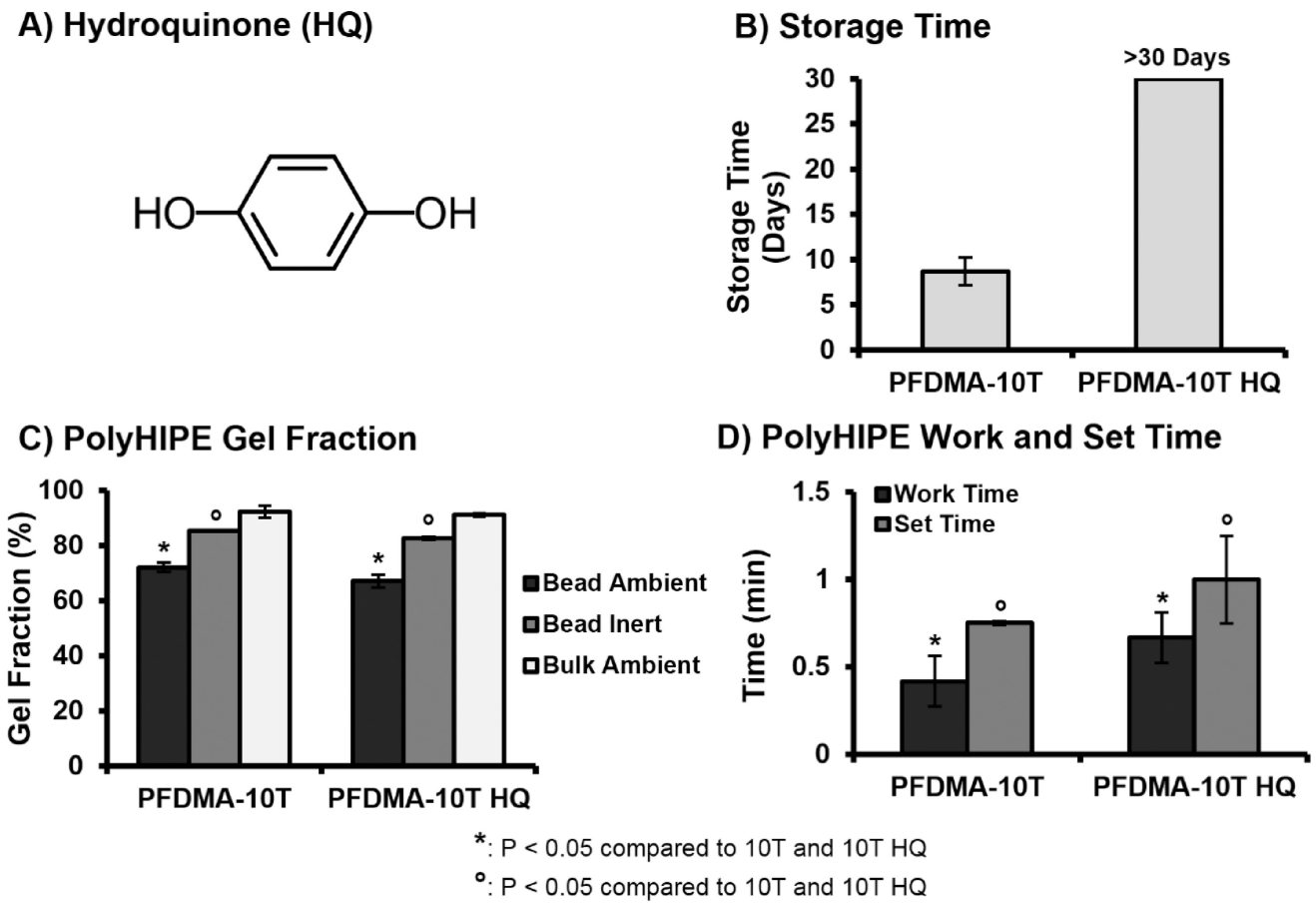

Figure 5.

The effect of hydroquinone inhibitor (A) on average storage time (B), work and set time (C), and gel fraction (D) of thiol-methacrylate polyHIPEs.

Author Manuscript Author Manuscript Author Manuscript Author Manuscript

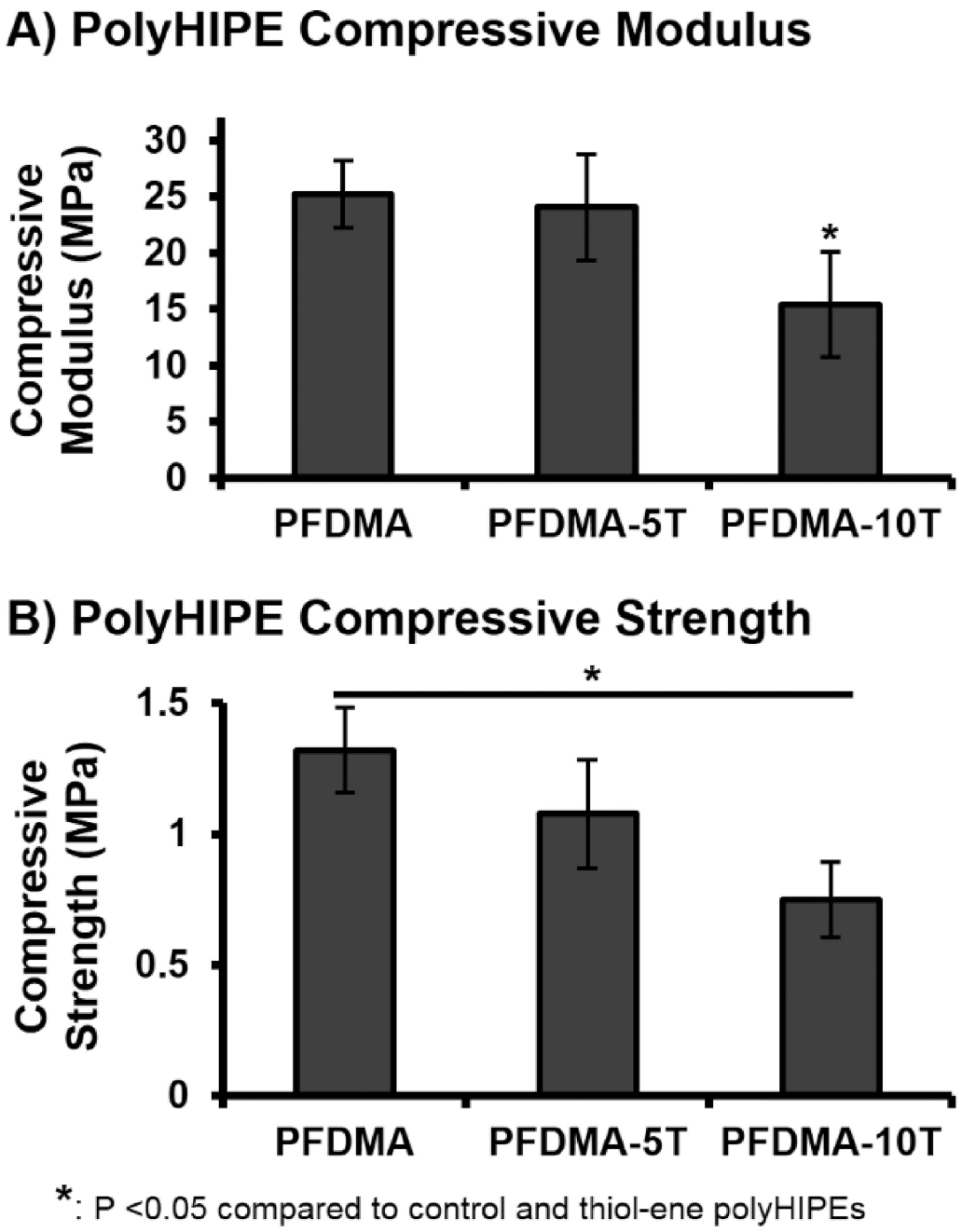

Figure 6.
The effect of increasing tetrathiol concentration on polyHIPE compressive modulus (A) and yield strength (B).

Author Manuscript Author Manuscript Author Manuscript Author Manuscript

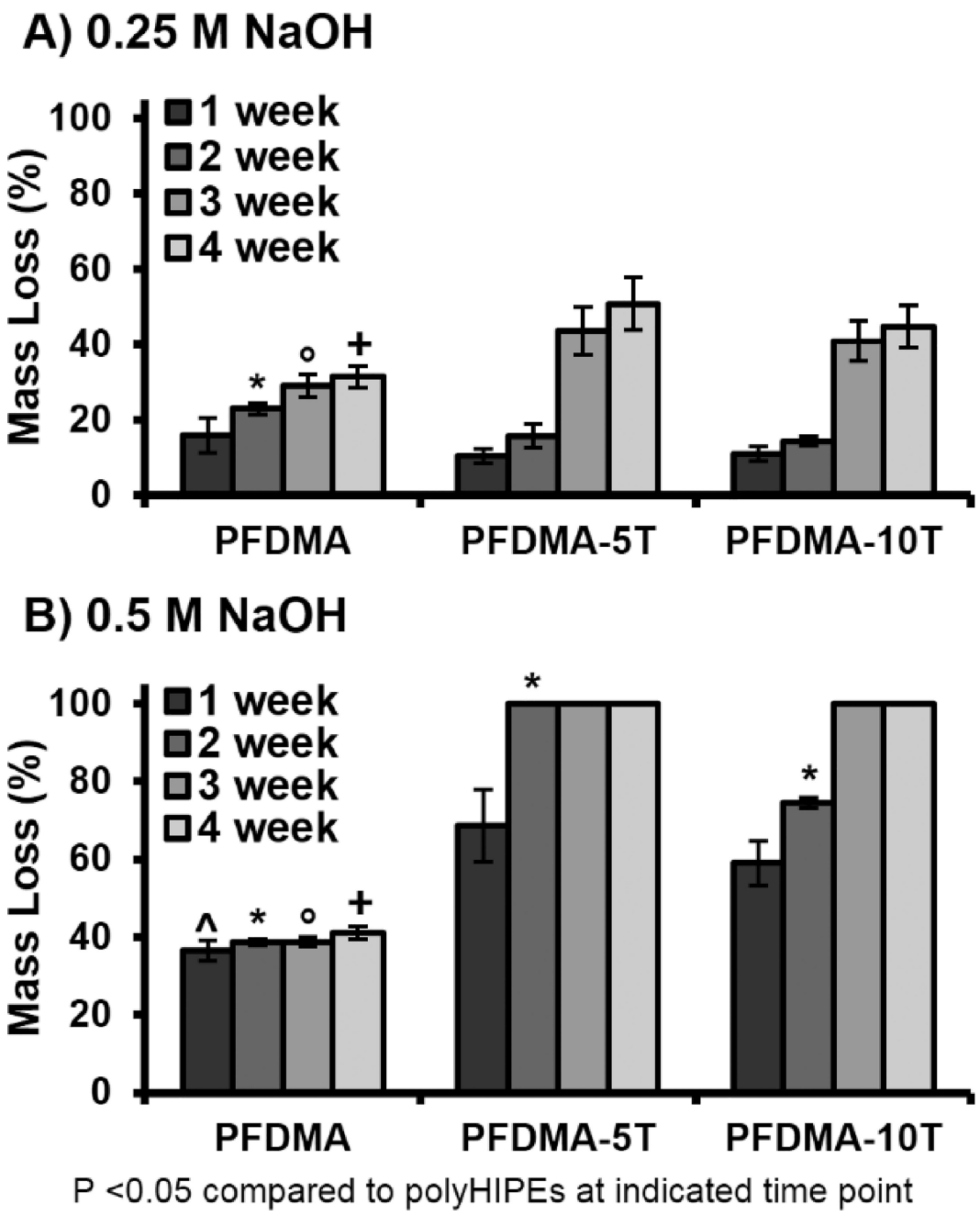

Figure 7.
The effect of increasing tetrathiol concentration on polyHIPE degradation up to 4 weeks in 0.25 M NaOH (A) and 0.5 M NaOH (B).

Author Manuscript Author Manuscript Author Manuscript Author Manuscript

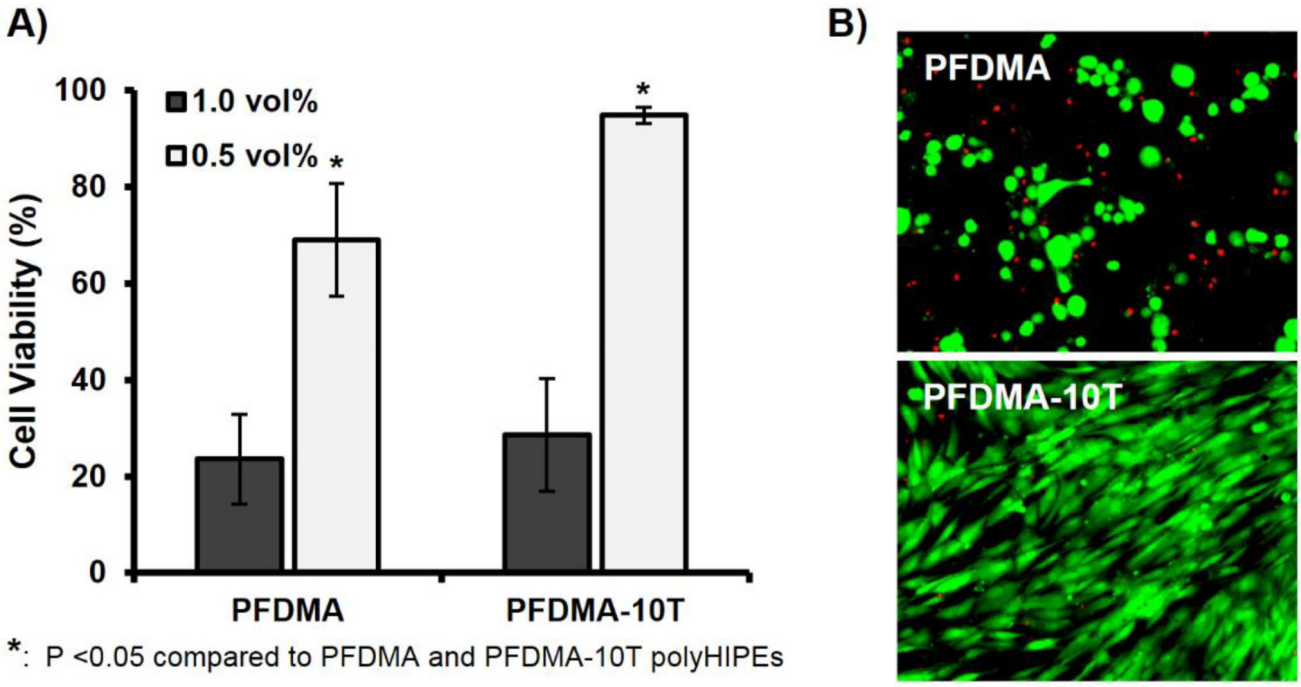

Figure 8.

hMSC viability after 24 h incubation with two concentrations of PFDMA and PFDMA-10T extracts (1.0 and 0.5 vol%) (A). Micrographs illustrating live (green) and dead (red) cells cultured with respective polyHIPE extracts at 0.5 vol% (B).

Author Manuscript Author Manuscript Author Manuscript Author Manuscript

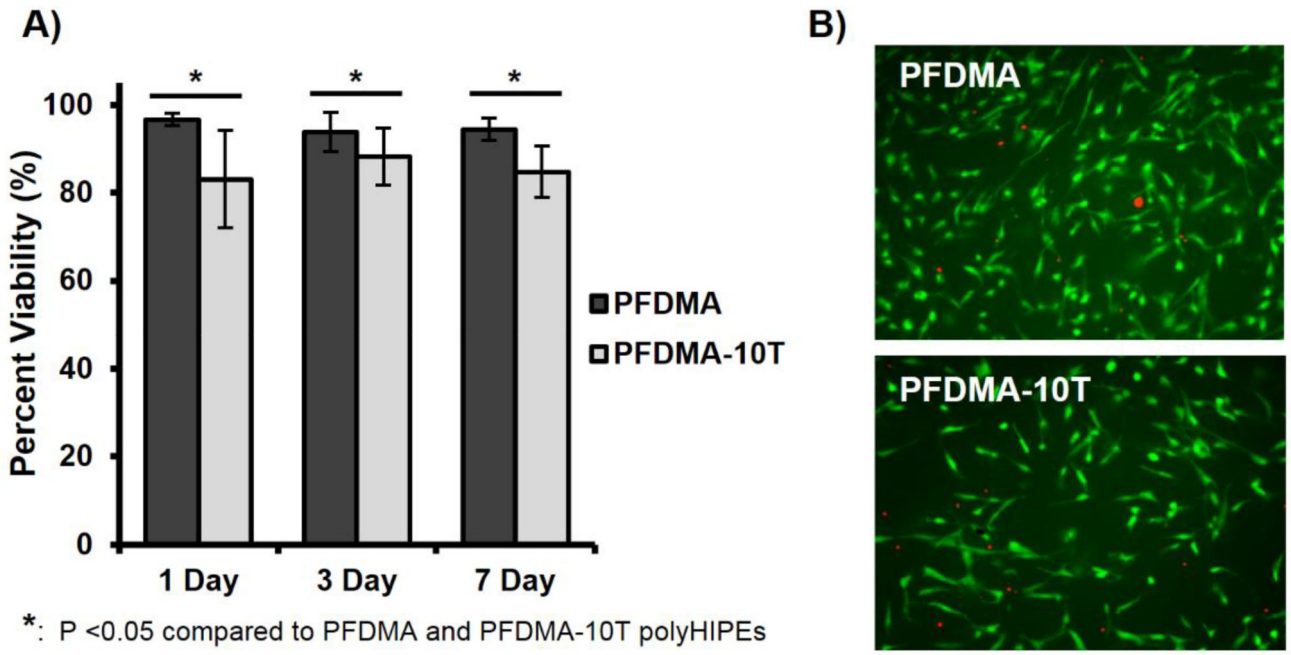

Figure 9.

hMSC viability on PFDMA and PFDMA-10T polyHIPEs at 1, 3, and 7 days (A). Micrographs illustrating live (green) and dead (red) cells on the respective polyHIPE sections at 7 days (B).

Author Manuscript Author Manuscript Author Manuscript Author Manuscript

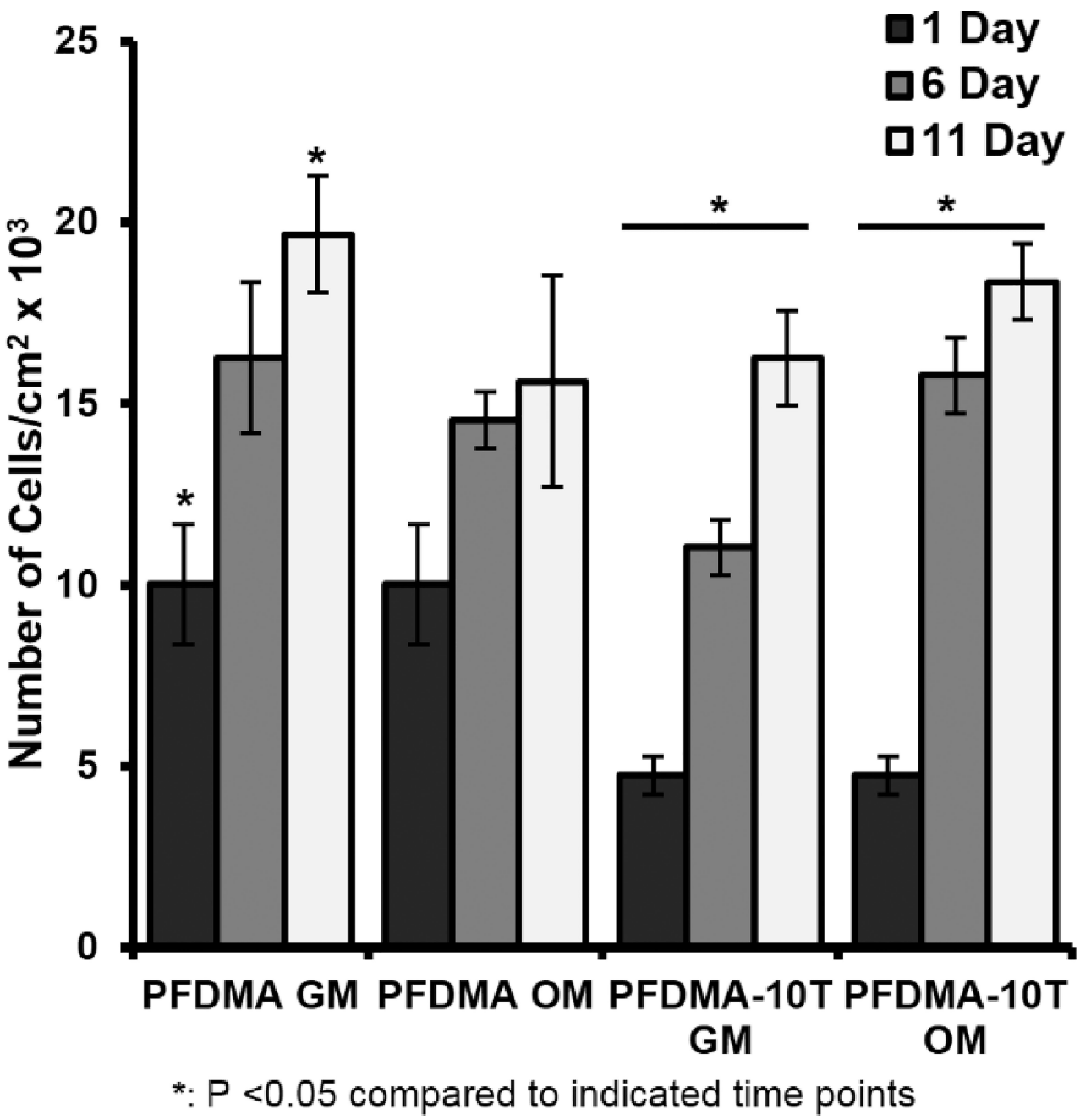

Figure 10.

Proliferation of hMSCs seeded on PFDMA and PFDMA-10T polyHIPEs at 1, 6, and 11 days as determined by DNA quantification. hMSCs were cultured in growth media (GM: 82.5% alpha MEM, 16.5% FBS, 1% L-glutamine) and osteogenic media (OM: growth media supplemented with 50 μg/mL ascorbic acid, 10 m*M* β-glycerophosphate, and 10 n*M* dexamethasone) with an initial cell seeding density was 50,000 cells/cm^2.

Author Manuscript Author Manuscript Author Manuscript Author Manuscript

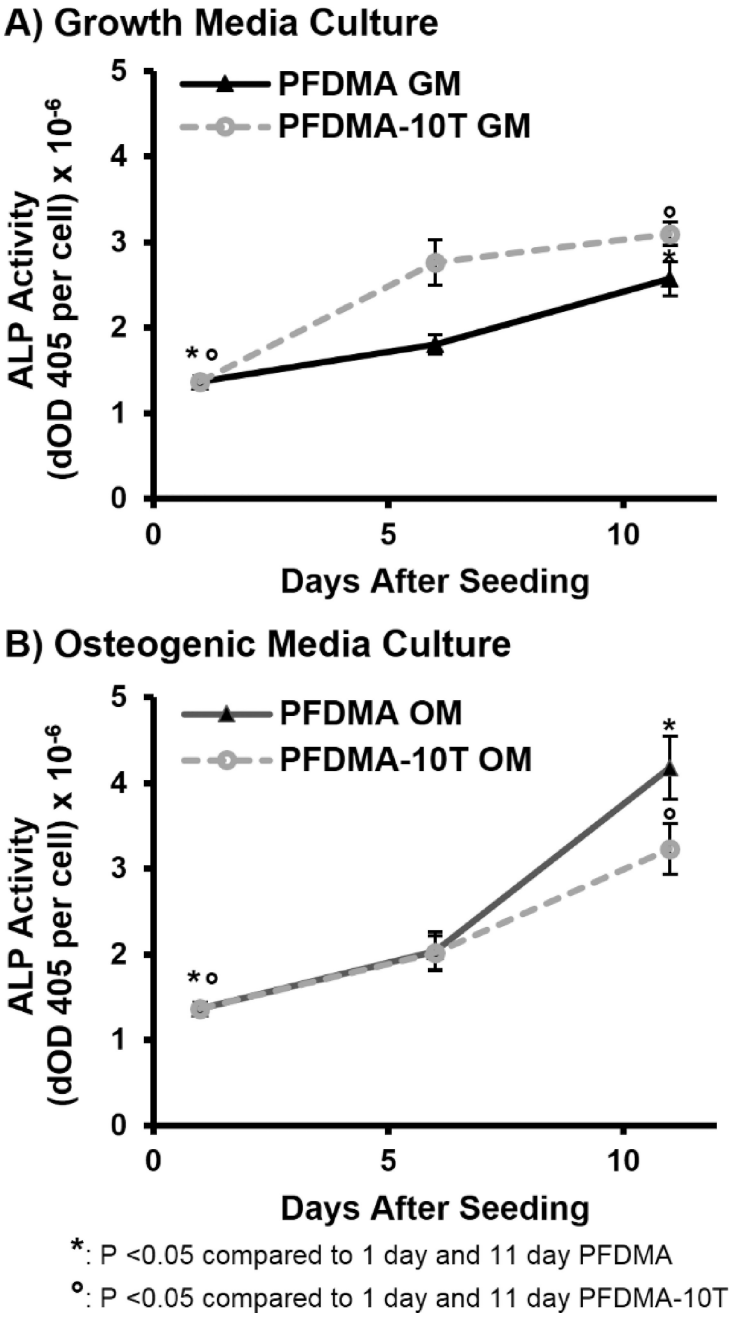

Figure 11.

Alkaline phosphatase activity of hMSCs seeded on PFDMA and PFDMA-10T polyHIPEs at 1, 6, and 11 days. PolyHIPEs were cultured in growth media (GM: 82.5% alpha MEM, 16.5% FBS, 1% L-glutamine) (A) and osteogenic media (OM: growth media supplemented with 50 μg/mL ascorbic acid, 10 m*M* β-glycerophosphate, and 10 n*M* dexamethasone) (B).